Search for Physics Beyond the Standard Model in Opposite-sign Dilepton Events in pp Collisions at $\sqrt{s} = 7$ TeV

The RA6 Crew...

Abstract

A search is presented for physics beyond the standard model (SM) in final states with opposite-sign isolated lepton pairs accompanied by hadronic jets and missing transverse energy. The search is performed using LHC data recorded with the CMS detector, corresponding to an integrated luminosity of 349 pb^{-1}. No evidence for an event yield beyond SM expectations is found. An upper limit on the non-SM contribution to the signal region is deduced from the results.

1 Introduction

In this note we describe a search for physics beyond the standard model (BSM) in a sample of proton-proton collisions at a centre-of-mass energy of 7 TeV. The data sample was collected with the Compact Muon Solenoid (CMS) detector [1] at the Large Hadron Collider (LHC) in 2011 and corresponds to an integrated luminosity of 349 pb^{-1}. This is an update of a previous analysis performed with a data sample of 34 pb^{-1} collected in 2010 [2].

The BSM signature in this search is motivated by three general considerations. First, new particles predicted by BSM physics scenarios are expected to be heavy, since they have so far eluded detection. Second, BSM physics signals with high enough cross sections to be observed in our current dataset are expected to be produced strongly, resulting in significant hadronic activity. Third, astrophysical evidence for dark matter suggests [3, 4] that the mass of weakly-interacting massive particles is of the order of the electroweak symmetry breaking scale. Such particles, if produced in pp collisions, could escape detection and give rise to an apparent imbalance in the event transverse energy. We therefore focus on the region of high missing transverse energy ($E_{\text{T}}^{\text{miss}}$). An example of a specific BSM scenario is provided by R-parity conserving supersymmetric (SUSY) models in which new, heavy particles are pair-produced and subsequently undergo cascade decays, producing hadronic jets and leptons [5, 6, 7, 8, 9, 10, 11]. These cascade decays may terminate in the production of weakly-interacting massive particles, resulting in large $E_{\text{T}}^{\text{miss}}$.

The results reported in this note are part of a broad program of BSM searches in events with jets and $E_{\text{T}}^{\text{miss}}$, characterized by the number and type of leptons in the final state. Here we describe a search for events containing opposite-sign isolated lepton pairs (e^+e^-, $e^\pm\mu^\mp$, $\mu^+\mu^-$) in addition to the jets and $E_{\text{T}}^{\text{miss}}$. Results from complementary searches with different final states have already been reported in Ref. [12] **ADD MORE REFS HERE**.

Our analysis strategy is as follows. In order to select dilepton events, we use high p_{T} dilepton triggers and a preselection based on that of the $t\bar{t}$ cross section measurement in the dilepton channel [13]. Good agreement is found between this data sample and predictions from SM Monte Carlo (MC) simulations in terms of the event yields and shapes of various kinematic distributions. We search for a kinematic edge in the dilepton mass distribution, which is a characteristic feature of SUSY models in which the opposite-sign leptons are produced via the decay $\chi_2^0 \to \chi_1^0 \ell^+ \ell^-$. Because BSM physics is expected to have large hadronic activity and $E_{\text{T}}^{\text{miss}}$ as discussed above, we proceed to define 2 signal regions with requirements on these quantities to select about 0.1% of dilepton $t\bar{t}$ events, as predicted by MC. We perform counting experiements in these signal regions, and compare the observed yields with the predictions from two independent background estimation techniques based on data control samples, as well as with SM and BSM MC expectations.

No specific BSM physics scenario, e.g. a particular SUSY model, has been used to optimize the search. In order to illustrate the sensitivity of the search, a simplified and practical model of SUSY breaking, the constrained minimal supersymmetric extension of the standard model (CMSSM) [14, 15], is used. The CMSSM is described by five parameters: the universal scalar and gaugino mass parameters (m_0 and $m_{1/2}$, respectively), the universal trilinear soft SUSY breaking parameter A_0, the ratio of the vacuum expectation values of the two Higgs doublets ($\tan\beta$), and the sign of the Higgs mixing parameter μ. Throughout the note, two CMSSM parameter sets, referred to as LM1 and LM3 [16], are used to illustrate possible CMSSM yields. The parameter values defining LM1 (LM3) are $m_0 = 60\ (330)\ \text{GeV}/c^2$, $m_{1/2} = 250\ (240)\ \text{GeV}/c^2$, $\tan\beta = 10\ (20)$ GeV; both LM1 and LM3 have $A_0 = 0$ and $\mu > 0$. These two scenarios are beyond the exclusion reach of previous searches performed at the Tevatron and LEP. The LM1 scenario was recently excluded by a search performed at CMS in events with jets and $E_{\text{T}}^{\text{miss}}$ [12]. In this analysis, the LM1 and LM3 scenarios serve as benchmarks which may be used to allow comparison of the sensitivity with other analyses.

2 CMS Detector

The central feature of the CMS apparatus is a superconducting solenoid, 13 m in length and 6 m in diameter, which provides an axial magnetic field of 3.8 T. Within the field volume are several particle detection systems. Charged particle trajectories are measured by silicon pixel and silicon strip trackers, covering $0 \leq \phi \leq 2\pi$ in azimuth and $|\eta| < 2.5$ in pseudorapidity, defined as $\eta = -\log[\tan\theta/2]$, where θ is the polar angle of the trajectory of the particle with respect to the counterclockwise proton beam direction. A crystal electromagnetic calorimeter and a brass/scintillator hadronic calorimeter surround the tracking volume, providing energy measurements of electrons and hadronic jets. Muons are identified and measured in gas-ionization detectors embedded in the steel return yoke outside the solenoid. The detector is nearly hermetic, allowing energy balance measurements in the plane transverse to the beam direction. A two-tier trigger system selects the most interesting pp collision events for use in physics analysis. A more detailed description of the CMS detector can be found elsewhere [1].

3 Event Selection

Samples of MC events are used to guide the design of the analysis. These events are generated using either the PYTHIA 6.4.22 [17] or MADGRAPH 4.4.12 [18] event generators. They are then simulated using a GEANT4-based model [19] of the CMS detector, and finally reconstructed and analyzed using the same software as is used to process collision data.

We apply a preselection based on that of the $t\bar{t}$ cross section measurement in the dilepton channel [13]. Events with two opposite-sign, isolated leptons (e^+e^-, $e^\pm\mu^\mp$, or $\mu^+\mu^-$) are selected. At least one of the leptons must have $p_{\rm T} > 20\,\text{GeV}/c$ and both must have $p_{\rm T} > 10\,\text{GeV}/c$, and the electrons (muons) must have $|\eta| < 2.5$ ($|\eta| < 2.4$). In events with more than two such leptons, the two leptons with the highest $p_{\rm T}$ are selected. Events with an e^+e^- or $\mu^+\mu^-$ pair with invariant mass between $76\,\text{GeV}/c^2$ and $106\,\text{GeV}/c^2$ or below $12\,\text{GeV}/c^2$ are removed, in order to suppress Drell–Yan (DY) $Z/\gamma^* \to \ell\ell$ events, as well as low mass dilepton resonances.

Events are required to pass at least one of a set of ee, $e\mu$ or $\mu\mu$ double-lepton triggers. The efficiency for events containing two leptons passing the analysis selection to pass at least one of these triggers is measured to be approximately 100%, 95%, and 90% for ee, $e\mu$ or $\mu\mu$ double-lepton triggers, respectively. In the following, the MC yields are weighted by these trigger efficiencies.

Because leptons produced in the decays of low-mass particles, such as hadrons containing b and c quarks, are nearly always inside jets, they can be suppressed by requiring the leptons to be isolated in space from other particles that carry a substantial amount of transverse momentum. The details of the lepton isolation measurement are given in Ref. [13]. In brief, a cone is constructed of size $\Delta R \equiv \sqrt{(\Delta\eta)^2 + (\Delta\phi)^2} = 0.3$ around the lepton momentum direction. The lepton relative isolation is then quantified by summing the transverse energy (as measured in the calorimeters) and the transverse momentum (as measured in the silicon tracker) of all objects within this cone, excluding the lepton, and dividing by the lepton transverse momentum. The resulting quantity is required to be less than 0.15, rejecting the large background arising from QCD production of jets.

We require the presence of at least two jets with $p_{\rm T} > 30\,\text{GeV}/c$ and $|\eta| < 3.0$, separated by $\Delta R > 0.4$ from leptons passing the analysis selection with $p_{\rm T} > 10\,\text{GeV}/c$. The anti-$k_T$ clustering algorithm [20] with $\Delta R = 0.5$ is used for jet clustering. The jets and $E_{\rm T}^{\rm miss}$ are reconstructed with the Particle Flow technique [28]. The event is required to satisfy $H_{\rm T} > 100\,\text{GeV}$, where $H_{\rm T}$ is defined as the scalar sum of the transverse energies of the selected jets. In addition, the $E_{\rm T}^{\rm miss}$ in the event is required to exceed 50 GeV.

The data yields and corresponding MC predictions after this event preselection are given in Table 1. The MC yields are normalized to $349\,\text{pb}^{-1}$ using next-to-leading order (NLO) cross sections. At the current LHC luminosity, the mean number of interactions in a single beam crossing is approximately 5. In the MC, multiple interactions are superimposed on the hard collision, and the MC is reweighted such that the distribution of reconstructed primary vertices matches that in data. As expected, the MC predicts that the sample passing the preselection is dominated by dilepton $t\bar{t}$. The data yield is in reasonable agreement with the prediction. We also quote the yields for the LM1 and LM3 benchmark scenarios.

Figure 1 compares several kinematic distributions in data and SM MC for events passing the preselection. As an illustration, we also show the MC distributions for the LM1 benchmark point. We find that the SM MC reproduces the properties of the bulk of dilepton $t\bar{t}$ events.

4 Search for a Kinematic Edge

Many models of new physics produce an excess of same flavor (SF) ee and $\mu\mu$ lepton pairs with respect to opposite flavor (OF) $e\mu$ pairs. For example, such an excess occurs in SUSY models in which the opposite-sign leptons are produced via the decay $\chi_2^0 \to \chi_1^0\ell^+\ell^-$. The kinematics of this decay also lead to a characteristic triangle-shaped feature in the distribution of dilepton mass, which would provide unambiguous evidence for new physics. In contrast, for the dominant background $t\bar{t}$, the flavors of the 2 leptons are uncorrelated, as is also the case for other SM background processes such as W^+W^- and DY$\to \tau^+\tau^-$. Therefore, for these processes the rates of SF and OF lepton pairs are the same modulo differences between the electron and muon selection efficiencies; furthermore, the kinematic properties of events containing SF and OF lepton pairs are the same. This allows us to determine the SM background in the SF final state using events in the OF final state; this technique is referred to as OF subtraction. In Sec. 5 we search for an excess of SF with respect to OF events accompanied by large $E_{\rm T}^{\rm miss}$ and H_T. In this section, we perform a fit to search for a kinematic edge in the dilepton mass distribution in SF events, in which we extract the background shape from OF events.

Table 1: Data yields and MC predictions after preselection, using the quoted NLO production cross sections σ. The $t\bar{t} \to \ell^+\ell^-$ corrresponds to dilepton $t\bar{t}$, including $t \to W \to \tau \to \ell$; $t\bar{t} \to$ fake includes all other $t\bar{t}$ decay modes. The samples of MC $t\bar{t}$, $W^{\pm}$ + jets, and single-top events were generated with MADGRAPH. The Drell–Yan sample (which includes events with invariant masses as low as 10 GeV/c^2) was generated using a mixture of MADGRAPH and PYTHIA and includes decays to the $\tau^+\tau^-$ final state. All other samples were generated with PYTHIA. The LM1 and LM3 benchmark scenarios are defined in the text; the quoted σ values refer to the total production cross section for SUSY particles in these scenarios. Uncertainties are statistical only.

Sample	σ	ee	$\mu\mu$	$e\mu$	total
$t\bar{t} \to \ell^+\ell^-$	16.9	147.6 ± 3.2	166.4 ± 3.2	391.7 ± 5.1	705.8 ± 6.8
$t\bar{t} \to$ fake	140.6	4.5 ± 0.6	1.3 ± 0.3	8.1 ± 0.7	13.9 ± 1.0
DY	18417	6.6 ± 1.8	9.5 ± 2.1	13.4 ± 2.6	29.6 ± 3.8
W^+W^-	2.9	1.4 ± 0.2	1.5 ± 0.2	3.4 ± 0.2	6.3 ± 0.3
$W^{\pm}Z^0$	0.3	0.3 ± 0.0	0.4 ± 0.0	0.7 ± 0.1	1.3 ± 0.1
Z^0Z^0	4.3	0.1 ± 0.0	0.1 ± 0.0	0.2 ± 0.0	0.4 ± 0.0
single top	33	4.5 ± 0.2	5.0 ± 0.2	11.9 ± 0.3	21.4 ± 0.5
W + jets	28049	4.5 ± 1.9	0.0 ± 0.0	2.8 ± 1.7	7.3 ± 2.6
total SM MC		169.7 ± 4.2	184.3 ± 3.9	432.2 ± 6.0	786.1 ± 8.3
data		193	201	485	879
LM1	6.7	22.3 ± 0.6	24.8 ± 0.6	12.8 ± 0.4	59.9 ± 0.9
LM3	5.3	7.9 ± 0.3	9.6 ± 0.3	14.2 ± 0.4	31.7 ± 0.6

In order to further suppress DY, we increase the $E_{\mathrm{T}}^{\mathrm{miss}}$ requirement to $E_{\mathrm{T}}^{\mathrm{miss}} > 100$ GeV. We search for the kinematic edge in 2 regions. The first region is a control region defined as $100 < H_T < 300$ GeV, which is dominated by the $t\bar{t}$ background; we use this region to validate our fit methodology and verify that a signal yield consistent with 0 is obtained. We then proceed to search for a kinematic edge in the signal region defined as $H_T > 300$ GeV. Since we do not observe a kinematic edge in this region, we perform a fit to the dilepton mass distribution assuming an example signal shape from the LM1 scenario. The residual DY background in the control region is fitted and extrapolated to the signal region where it is found to be very small.

The relative yields in the $e\mu$, ee and $\mu\mu$ channels are constrained using $R_{\mu e} = 1.13 \pm 0.05$ (the ratio of muon to electron selection efficiencies), evaluated by taking the square root of the ratio of the number of $Z \to \mu^+\mu^-$ to $Z \to e^+e^-$ events in data, in the mass range 76-106 GeV with no jets or $\not\!\!E_T$ requirements.

The background as a function of the invariant mass $m_{\ell\ell}$ is described by:

$$B(m_{\ell\ell}) = m_{\ell\ell}^{a} e^{-b m_{\ell\ell}}, \tag{1}$$

where $a \approx 1.5$ describes the rising edge and $b \approx 0.003$ dominates the long exponential tail on the right hand side of the shape. The extracted shape compared to the dilepton mass distribution in the control region for events containing OF lepton pairs is shown in Fig. 2 (upper-right).

For a potential signal, we use an edge model for a two-body decay, which comprises a triangular shape convoluted with a gaussian, according to:

$$T(m_{\ell\ell}) = \frac{1}{\sqrt{2\pi}\sigma} \int_0^{M_{cut}} dy\; y e^{\frac{(-(m_{\ell\ell}-y)^2}{2\sigma^2}}, \tag{2}$$

where the resolution parameters for electrons σ_{ee} and muons $\sigma_{\mu\mu}$ are constrained based on simulation.

The position of the kinematic edge M_{cut} is fixed based on the generator level information for the signal model which is tested; for example, for LM1 $M_{cut} = 77.8$ GeV. Finally, the Z contribution is modelled by a Breit-Wigner convoluted with a Gaussian (with fixed Z mass and width).

We perform a simultaneous, extended, unbinned maximum likelihood (ML) fit to the distribution of dilepton mass for events containing ee, $\mu\mu$ (signal, Z and background model) and $e\mu$ pairs (background model only). The shape of the $t\bar{t}$ background shape is assumed to be common in all categories and the yields of signal n_S, Z n_Z and background n_B in the three categories are constrained using $R_{\mu e}$.

We perform the fit in the control region $100 < H_T < 300$ GeV, in which the $t\bar{t}$ background, Z background,

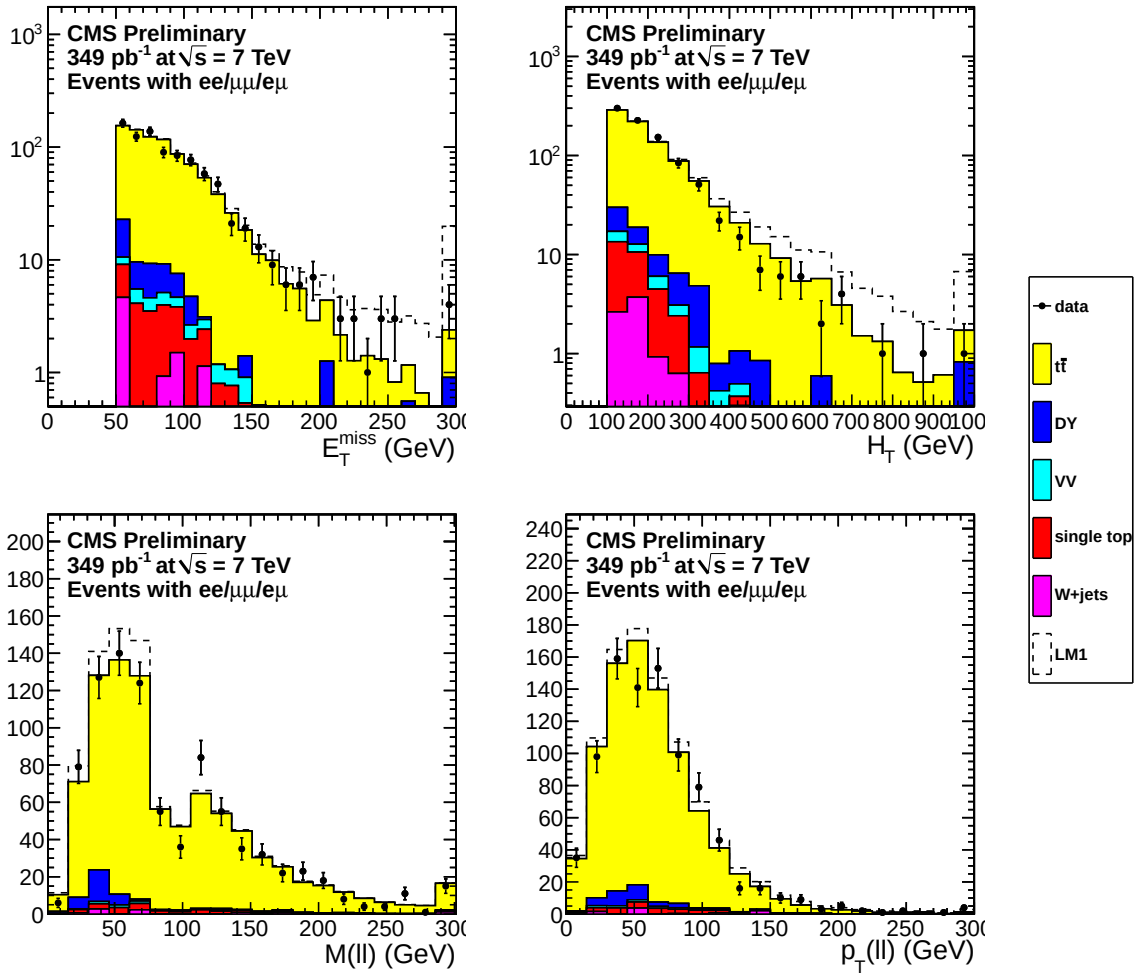

Figure 1: Distributions of (top left) missing tranverse energy $E_{\mathrm{T}}^{\mathrm{miss}}$, (top right) scalar sum of jet transverse energies (H_{T}), (bottom left) dilepton invariant mass $M(\ell\ell)$, and (bottom right) dilepton transverse momentum $p_{\mathrm{T}}(\ell\ell)$ for SM MC and data after preselection. The last bin contains the overflow. The MC has been normalized to match the data by applying a scale factor of 1.12. Here VV indicates the sum of WW, WZ, and ZZ. The MC distributions for the LM1 benchmark point are also shown.

and LM1 signal yields are allowed to vary in the fit. The extracted signal yield, constrained to be positive, is $n_S = 0.0 \pm 7.3$, consistent with the background only hypothesis, as displayed in Fig. 2 (upper-left). The extracted Z yield is $n_Z = 5.2 \pm 4.2$, which is used to constrain the Z yield in the signal region.

Next, we perform the fit in the signal region $H_T > 300$ GeV. The $t\bar{t}$ shape overlaid over OF events is shown in Fig. 2 (lower-right). We constrain the Z yield in this region using an extrapolation in H_T from the control region $100 < H_T < 300$ GeV. The Z yield in the control region is multiplied by a scale factor derived from Z events in data with no requirement on $E_{\mathrm{T}}^{\mathrm{miss}}$, which quantifies the fraction of Z events with $H_T > 100$ GeV which satisfy $H_T > 300$ GeV. Using this procedure we derive an upper limit on the Z yield in the signal region of $n_Z < 0.5$, which we use to constrain the Z yield in the ML fit. The extracted signal yield is $n_S = 3.5 \pm 4.9$, which is consistent with the background only hypothesis, as shown in Fig. 2 (lower-left). The expected LM1 yield in this region is 23 ± 2 events.

5 Counting Experiments

To look for possible BSM contributions, we define 2 signal regions that preserve about 0.1% of the dilepton $t\bar{t}$ events, by adding requirements of large $E_{\mathrm{T}}^{\mathrm{miss}}$ and H_T:

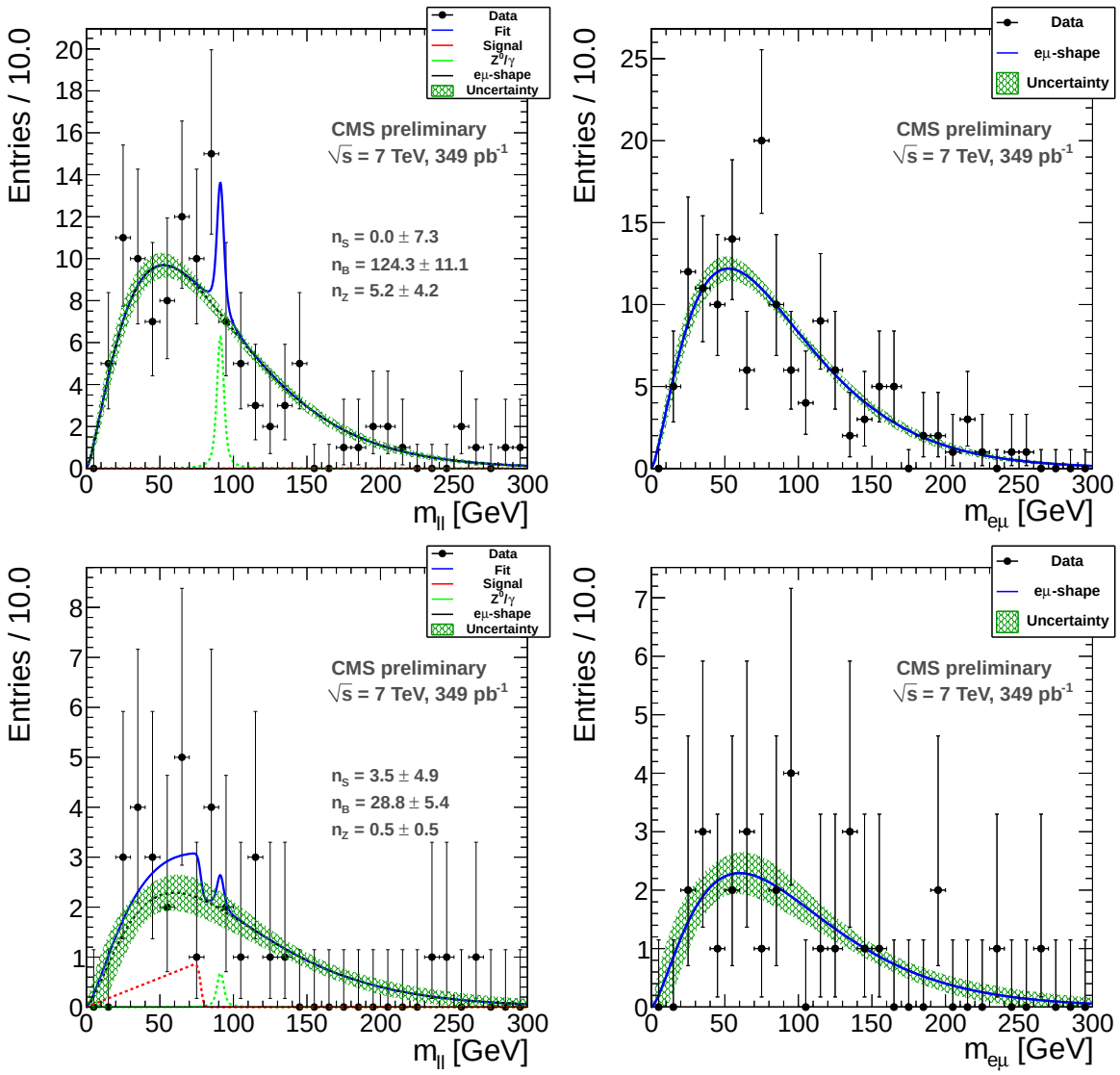

Figure 2: Results of the maximum likelihood fit to the dilepton mass distribution for events containing ee and $\mu\mu$ lepton pairs (left) and $e\mu$ lepton pairs (right) in the control region defined as $100 < H_T < 300$ GeV, $E_{\mathrm{T}}^{\mathrm{miss}} > 100$ GeV (upper) and the signal region $H_T > 300$ GeV, $E_{\mathrm{T}}^{\mathrm{miss}} > 100$ GeV (lower). In the extended fit the number of signal n_S, Z n_Z and $t\bar{t}$ n_B events is extracted as well.

- high $E_{\mathrm{T}}^{\mathrm{miss}}$ signal region: $E_{\mathrm{T}}^{\mathrm{miss}} > 275$ GeV, $H_T > 300$ GeV,
- high H_T signal region: $E_{\mathrm{T}}^{\mathrm{miss}} > 200$ GeV, $H_T > 600$ GeV.

For the high $E_{\mathrm{T}}^{\mathrm{miss}}$ (high H_T) signal region, the MC predicts 2.6 (2.5) SM events, dominated by dilepton $t\bar{t}$; the expected LM1 yield is 17 (14) and the expected LM3 yield is 6.4 (6.7). The signal regions are indicated in Fig. 3. These signal regions are tighter than the one used in our published 2010 analysis since with the larger data sample they give improved sensitivity to contributions from new physics.

We perform counting experiments in these signal regions, and use three independent methods to estimate from data the background in the signal region. The first method is a novel technique based on the ABCD method, which we used in our 2010 analysis [2], and exploits the fact that H_{T} and $y \equiv E_{\mathrm{T}}^{\mathrm{miss}}/\sqrt{H_T}$ are nearly uncorrelated for the $t\bar{t}$ background; this method is referred to as the ABCD' technique. First, we extract the y and H_T distributions $f(y)$ and $g(H_T)$ from data, using events from control regions which are dominated by background. Because y and H_T are weakly-correlated, the distribution of events in the y vs. H_T plane is described by:

$$\frac{\partial^2 N}{\partial y \partial H_T} = f(y)g(H_T), \tag{3}$$

allowing us to deduce the number of events falling in any region of this plane. In particular, we can deduce the number of events falling in our signal regions defined by requirements on $E_{\mathrm{T}}^{\mathrm{miss}}$ and H_T.

We measure the $f(y)$ and $g(H_T)$ distributions using events in the regions indicated in Fig. 4, and predict the background yields in the signal regions using Eq. 3. To estimate the statistical uncertainty in the predicted background, the bin contents of $f(y)$ and $g(H_T)$ are smeared according to their Poisson uncertainties, the prediction is repeated 20 times with these smeared distributions, and the RMS of the deviation from the nominal prediction is taken as the statistical uncertainty. We have studied this technique using toy MC studies based on event samples of similar size to the expected yield in data for 1 fb^{-1}. Based on these studies we correct the predicted background yields by factors of 1.2 ± 0.5 (1.0 ± 0.5) for the high $E_{\mathrm{T}}^{\mathrm{miss}}$ (high H_T) signal region.

The second background estimate, henceforth referred to as the dilepton transverse momentum ($p_{\mathrm{T}}(\ell\ell)$) method, is based on the idea [23] that in dilepton $t\bar{t}$ events the p_{T} distributions of the charged leptons and neutrinos from W decays are related, because of the common boosts from the top and W decays. This relation is governed by the polarization of the W's, which is well understood in top decays in the SM [24, 25] and can therefore be reliably accounted for. We then use the observed $p_{\mathrm{T}}(\ell\ell)$ distribution to model the $p_{\mathrm{T}}(\nu\nu)$ distribution, which is identified with $E_{\mathrm{T}}^{\mathrm{miss}}$. Thus, we use the number of observed events with $H_{\mathrm{T}} > 300\,\mathrm{GeV}$ and $p_{\mathrm{T}}(\ell\ell) > 275\,\mathrm{GeV}$ ($H_{\mathrm{T}} > 600\,\mathrm{GeV}$ and $p_{\mathrm{T}}(\ell\ell) > 200\,\mathrm{GeV}$) to predict the number of background events with $H_{\mathrm{T}} > 300\,\mathrm{GeV}$ and $E_{\mathrm{T}}^{\mathrm{miss}} > 275\,\mathrm{GeV}$ ($H_{\mathrm{T}} > 600\,\mathrm{GeV}$ and $E_{\mathrm{T}}^{\mathrm{miss}} > 200\,\mathrm{GeV}$). In practice, we apply two corrections to this prediction, following the same procedure as in Ref. [2]. The first correction is $K_{50} = 1.5 \pm 0.3$ (1.3 ± 0.2) for the high $E_{\mathrm{T}}^{\mathrm{miss}}$ (high H_T) signal region. The second correction factor is $K_C = 1.5 \pm 0.5$ (1.3 ± 0.4) for the high $E_{\mathrm{T}}^{\mathrm{miss}}$ (high H_T) signal region.

Our third background estimation method is based on the fact that many models of new physics produce an excess of SF with respect to OF lepton pairs, while for the $t\bar{t}$ background the rates of SF and OF lepton pairs are the same. Hence we make use of the OF subtraction technique discussed in Sec. 4 in which we performed a shape analysis of the dilepton mass distribution. Here we perform a counting experiment, by quantifying the the excess of SF vs. OF pairs using the quantity

$$\Delta = R_{\mu e} N(ee) + \frac{1}{R_{\mu e}} N(\mu\mu) - N(e\mu). \tag{4}$$

This quantity is predicted to be 0 for processes with uncorrelated lepton flavors. In order for this technique to work, the kinematic selection applied to events in all dilepton flavor channels must be the same, which is not the case for our default selection because the Z mass veto is applied only to same-flavor channels. Therefore when applying the OF subtraction technique we also apply the Z mass veto to the $e\mu$ channel.

All background estimation methods based on data are in principle subject to signal contamination in the control regions, which tends to decrease the significance of a signal which may be present in the data by increasing the background prediction. In general, it is difficult to quantify these effects because we do not know what signal may be present in the data. Having three independent methods (in addition to expectations from MC) adds redundancy because signal contamination can have different effects in the different control regions for the three methods. For example, in the extreme case of a BSM signal with identical distributions of $p_{\mathrm{T}}(\ell\ell)$ and $E_{\mathrm{T}}^{\mathrm{miss}}$, an excess of events might be seen in the ABCD' method but not in the $p_{\mathrm{T}}(\ell\ell)$ method.

Backgrounds in which one or both leptons do not originate from electroweak decays (non-W/Z leptons) are assessed using the method of Ref. [13]. A non-W/Z lepton is a lepton candidate originating from within a jet, such as a lepton from semileptonic b or c decays, a muon decay-in-flight, a pion misidentified as an electron, or an unidentified photon conversion. Estimates of the contributions to the signal region from pure multijet QCD, with two non-W/Z leptons, and in $W + \mathrm{jets}$, with one non-W/Z lepton in addition to the lepton from the decay of the W, are derived separately. We find $0.00^{+0.04}_{-0.00}$ and $0.0^{+0.5}_{-0.0}$ ($0.00^{+0.04}_{-0.00}$ and 0.5 ± 0.5) for the multijet QCD and W+jets contributions to the high $E_{\mathrm{T}}^{\mathrm{miss}}$ (high H_T) signal regions, respectively, and thus consider these backgrounds to be negligible.

Backgrounds from DY are estimated with the data-driven $R_{out/in}$ technique [13], which leads to an estimated DY contribution which is consistent with 0. Backgrounds from processes with two vector bosons and single top are negligible compared to dilepton $t\bar{t}$.

6 Results

The data is displayed in the plane of $E_{\mathrm{T}}^{\mathrm{miss}}$ vs. H_T in Fig. 3. We find 4 (3) events in the high $E_{\mathrm{T}}^{\mathrm{miss}}$ (high H_T) signal regions, consistent with the MC expectations.

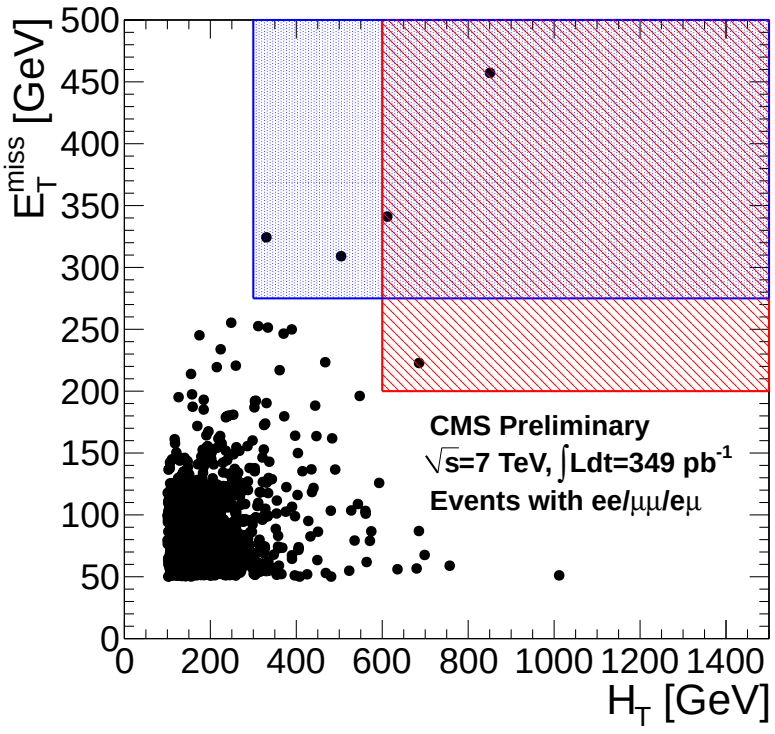

Figure 3: Distributions of $E_{\mathrm{T}}^{\mathrm{miss}}$ vs. H_{T} for data. The high $E_{\mathrm{T}}^{\mathrm{miss}}$ (high H_T) signal region is indicated with the blue dotted (red striped) region.

Next, we apply the ABCD' method to predict the yields in the high $\not\!\!E_T$ and high H_T signal regions. The y vs. H_T distributions for data are displayed in Fig. 4. The signal regions are indicated, as well as the control regions used to measure the $f(y)$ and $g(H_T)$ distributions. For the high $\not\!\!E_T$ signal region, we find a predicted yield of 1.2 ± 0.4 (stat) $\pm$ 0.5 (syst), in reasonable agreement with the MC prediction. For the high H_T signal region, we do not find any events in the control region used to extract $g(H_T)$ with $H_T > 600$ GeV, and the ABCD' background estimate is therefore 0. To assess the statistical uncertainty in this prediction, we add a single event "by hand" to the $g(H_T)$ distributiion at $H_T = 600$ GeV, leading to a predicted yield of 0.0 ± 0.6 (stat) $\pm$ 0.3 (syst).

Next, we use the $p_T(\ell\ell)$ template method to predict the background in the 2 signal regions. For each signal region S, we count the number of events falling in the region S', which is defined using the same requirements as S but replacing the $E_{\mathrm{T}}^{\mathrm{miss}}$ requirement with a $p_T(\ell\ell)$ requirement. We subtract off the expected DY contribution using the data-driven $R_{out/in}$ technique. We scale this yield by the 2 corrections factors: K_{50} and K_C of Sec. 5.

The predicted and observed $E_{\mathrm{T}}^{\mathrm{miss}}$ distributions in the 2 signal regions are displayed in Fig. 5. For the high $E_{\mathrm{T}}^{\mathrm{miss}}$ (high H_T) signal regions we predict a background yield of 5.4 ± 3.8 (stat) $\pm$ 2.2 (syst) (1.7 ± 1.7 (stat) $\pm$ 0.6 (syst)) events, consistent with the observed yields and with the predictions of the ABCD' method.

As a validation of the $p_{\mathrm{T}}(\ell\ell)$ method in a region which is dominated by background, we also apply the $p_{\mathrm{T}}(\ell\ell)$ method in a control region by restricting H_{T} to be in the range 125–300 GeV. Here we predict 6.5 ± 4.4 events with $E_{\mathrm{T}}^{\mathrm{miss}} > 200$ GeV, and observe 6 events in this region.

Our third background estimate is based on the OF subtraction technique. We observe 2 ee + 1 $e\mu$ (1 ee + 1 $e\mu$) events in the high $E_{\mathrm{T}}^{\mathrm{miss}}$ (high H_T) signal regions outside of the Z mass region 76–106 GeV. This gives $\Delta = 1.3$ $\pm$ 1.9 (stat) $\pm$ 0.1 (syst) (0.1 ± 1.5 (stat) $\pm$ 0.0 (syst)) for the high $E_{\mathrm{T}}^{\mathrm{miss}}$ (high H_T) signal regions, respectively.

A summary of our results is presented in Table 2. For both signal regions, the observed yield is consistent with the predictions from MC and from the background estimates based on data. We conclude that no evidence for non-SM contributions to the signal regions is observed.

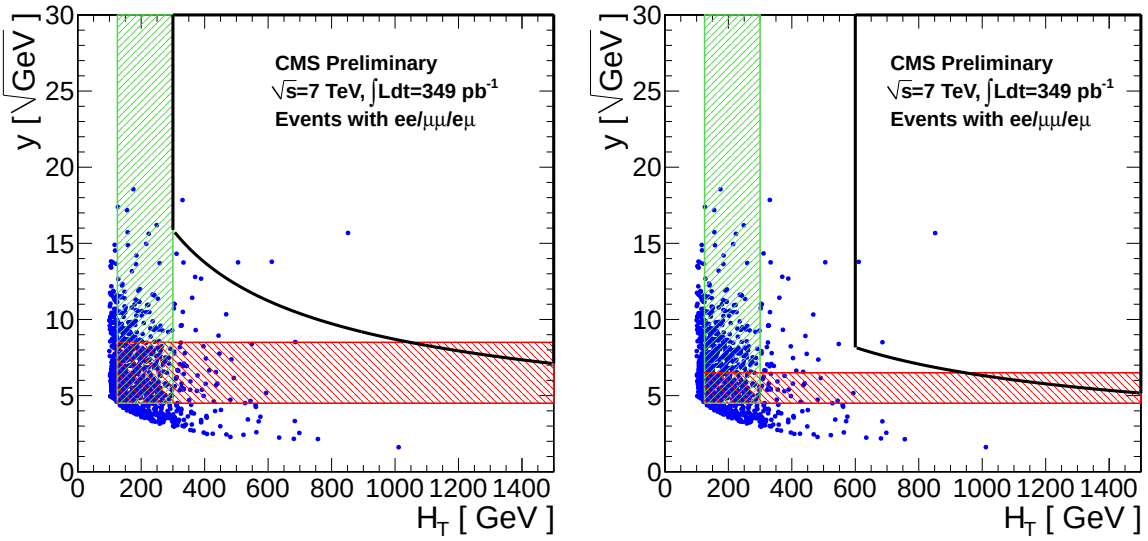

Figure 4: Distributions of y vs. H_T in data. The signal regions $\not\!\!E_T > 275$ GeV, $H_T > 300$ GeV (left) and $\not\!\!E_T > 200$ GeV, $H_T > 600$ GeV (right) are indicated with thick black lines. The $f(y)$ and $g(H_T)$ functions are measured using events in the green and red shaded areas, respectively.

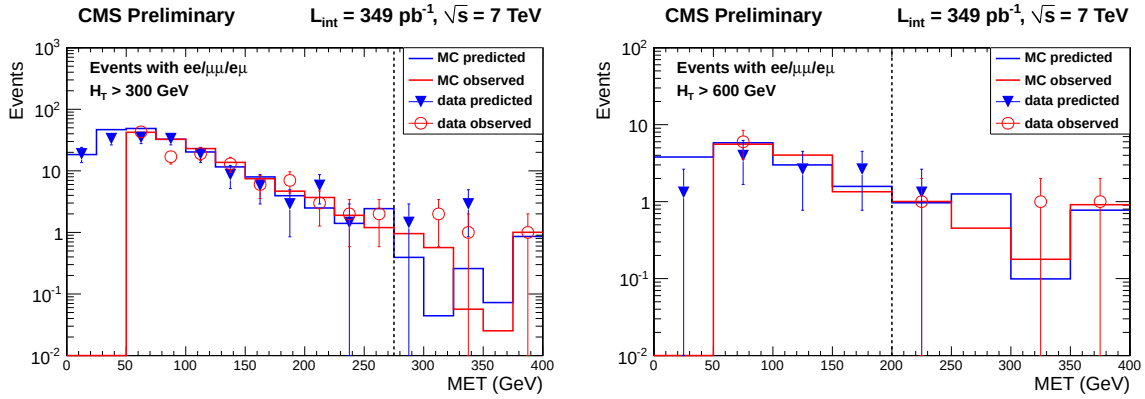

Figure 5: Distributions of $p_T(\ell\ell)$ scaled by the $E_{\rm T}^{\rm miss}$ acceptance correction factor K (predicted) and $\not\!\!E_T$ (observed) for SM MC and data. The high $E_{\rm T}^{\rm miss}$ (high H_T) signal region is indicated by the vertical line in the left (right) plot.

7 Acceptance and Efficiency Systematic Uncertainties

The acceptance and efficiency, as well as the systematic uncertainties in these quantities, depend on the signal model. For some of the individual uncertainties, it is reasonable to quote values based on SM control samples with kinematic properties similar to the SUSY benchmark models. For others that depend strongly on the kinematic properties of the event, the systematic uncertainties must be quoted model by model.

The systematic uncertainty in the lepton acceptance consists of two parts: the trigger efficiency uncertainty and the identification and isolation uncertainty. The trigger efficiency for two leptons of $p_{\rm T} > 10\,\text{GeV}/c$, with one lepton of $p_{\rm T} > 20\,\text{GeV}/c$ is measured to be approximately 100%, 90% and 95% for events with ee, $\mu\mu$ and $e\mu$ leptons using samples of $Z \to \ell\ell$, with an uncertainty of 2%. We verify that the MC reproduces the lepton identification and isolation efficiencies in data using samples of $Z \to \ell\ell$; the data and MC efficiencies are found to be consistent within 2%.

Another significant source of systematic uncertainty is associated with the jet and $E_{\rm T}^{\rm miss}$ energy scale. The impact of this uncertainty is final-state dependent. Final states characterized by very large hadronic activity and $E_{\rm T}^{\rm miss}$ are less sensitive than final states where the $E_{\rm T}^{\rm miss}$ and $H_{\rm T}$ are typically close to the minimum requirements applied to these quantities. To be more quantitative, we have used the method of Ref. [13] to evaluate the systematic uncertainties in the acceptance for $t\bar{t}$ and for the two benchmark SUSY points using a 5% uncertainty in the hadronic energy

scale [26]. The uncertainty on the LM1 signal efficiency in the region $H_T > 300$ GeV, $E_{\mathrm{T}}^{\mathrm{miss}} > 100$ GeV used to search for the kinematic edge is 3%. For the high $E_{\mathrm{T}}^{\mathrm{miss}}$ signal region for $t\bar{t}$ the uncertainty is 35%; for LM1 and LM3 the uncertainties are 14% and 18%, respectively. For the high H_T signal region for $t\bar{t}$ the uncertainty is 30%; for LM1 and LM3 the uncertainties are 20% and 21%, respectively.

The uncertainty in the integrated luminosity is 4% [27].

8 Limits on New Physics

We set an upper limit on the signal yield extracted by the fit to the dilepton mass distribution, assuming the LM1 shape. The 95% confidence level (CL) upper limit (UL) is extracted using a profile likelihood technique, giving an UL of 14.3 events, including uncertainties in the background yield and shape, resolution model and Z yield. In the limit setting we also include the uncertainties from trigger efficiency, lepton selection efficiency, hadronic energy scale and integrated luminosity on the signal efficiency. The expected LM1 yield is 23 ± 2 events.

We set upper limits on the non-SM contributions to the high $E_{\mathrm{T}}^{\mathrm{miss}}$ and high H_T signal regions. For both regions, we find reasonable agreement between the observed yields and the predictions from MC and from the 2 data-driven methods. We choose here to extract the upper limits using the MC prediction for the background estimate. The 95% CL upper limit is extracted using a Bayesian technique [29], with a log-normal model of nuissance parameter integration assuming 0 signal. The results are summarized in Table 2.

Table 2: Summary of the observed and predicted yields in the 2 signal regions. The uncertainty in the MC prediction is statistical only. The systematic uncertainties on the ABCD', $p_T(\ell\ell)$, and OF subtraction predictions are discussed in the text. The non-SM yield UL is a Bayesian 95% confidence level upper limit. The LM1 and LM3 yields include uncertainties from trigger efficiency, lepton selection efficiency, hadronic energy scale and integrated luminosity.

	high $\not\!\!E_T$ signal region	high H_T signal region
Observed yield	4	3
MC prediction	2.6 ± 0.8	2.5 ± 0.8
ABCD' prediction	1.2 ± 0.4 (stat) ± 0.5 (syst)	0.0 ± 0.6 (stat) ± 0.3 (syst)
$p_T(\ell\ell)$ prediction	5.4 ± 3.8 (stat) ± 2.2 (syst)	1.7 ± 1.7 (stat) ± 0.6 (syst)
non-SM yield UL	5.2	4.1
LM1 yield	17 ± 2.5	14 ± 2.9
LM3 yield	6.4 ± 1.2	6.7 ± 1.5
OF subtraction (Δ)	1.3 ± 1.9 (stat) ± 0.1 (syst)	0.1 ± 1.5 (stat) ± 0.0 (syst)

9 Summary

We have presented a search for BSM physics in the opposite-sign dilepton final state using a data sample of proton-proton collisions at 7 TeV centre-of-mass energy corresponding to an integrated luminosity of 349 pb^{-1}, recorded by the CMS detector in 2011. The search focused on dilepton events with large missing transverse energy and significant hadronic activity, motivated by many models of BSM physics, such as supersymmetric models. Good agreement with standard model predictions was found, both in terms of event yields and shapes of various relevant kinematic distributions. In the absence of evidence for BSM physics, we have set upper limits on the non-SM contributions to the signal regions.

Acknowledgments

We wish to congratulate our colleagues in the CERN accelerator departments for the excellent performance of the LHC machine. We thank the technical and administrative staff at CERN and other CMS institutes, and acknowledge support from: FMSR (Austria); FNRS and FWO (Belgium); CNPq, CAPES, FAPERJ, and FAPESP (Brazil); MES (Bulgaria); CERN; CAS, MoST, and NSFC (China); COLCIENCIAS (Colombia); MSES (Croatia); RPF (Cyprus); Academy of Sciences and NICPB (Estonia); Academy of Finland, ME, and HIP (Finland); CEA and CNRS/IN2P3 (France); BMBF, DFG, and HGF (Germany); GSRT (Greece); OTKA and NKTH (Hungary); DAE and DST (India); IPM (Iran); SFI (Ireland); INFN (Italy); NRF and WCU (Korea); LAS (Lithuania); CINVESTAV, CONACYT, SEP, and UASLP-FAI (Mexico); PAEC (Pakistan); SCSR (Poland); FCT (Portugal); JINR (Armenia,

Belarus, Georgia, Ukraine, Uzbekistan); MST and MAE (Russia); MSTD (Serbia); MICINN and CPAN (Spain); Swiss Funding Agencies (Switzerland); NSC (Taipei); TUBITAK and TAEK (Turkey); STFC (United Kingdom); DOE and NSF (USA).

References

[1] **CMS** Collaboration, R. Adolphi et al., "The CMS experiment at the CERN LHC", *JINST* **3** (2008) S08004. doi:10.1088/1748-0221/3/08/S08004.

[2] arXiv:1103.1348v1 [hep-ex], "Search for Physics Beyond the Standard Model in Opposite-Sign Dilepton Events at $\sqrt{s} = 7$ TeV."

[3] G. Bertone, D. Hooper, and J. Silk, "Particle dark matter: Evidence, candidates and constraints", *Phys. Rept.* **405** (2005) 279–390. doi:10.1016/j.physrep.2004.08.031.

[4] H. Baer, "TASI 2008 lectures on Collider Signals II: missing E_T signatures and the dark matter connection", arXiv:hep-ph/0901.4732.

[5] S. P. Martin, "A Supersymmetry Primer", arXiv:hep-ph/9709356v5.

[6] Y. A. Golfand and E. P. Likhtman, "Extension of the Algebra of Poincare Group Generators and Violation of p Invariance", *JETP Lett.* **13** (1971) 323–326.

[7] J. Wess and B. Zumino, "Supergauge transformations in four dimensions", *Nucl. Phys.* **B70** (1974) 39. doi:10.1016/0550-3213(74)90355-1.

[8] H. P. Nilles, "Supersymmetry, Supergravity and Particle Physics", *Phys. Reports* **110** (1984) 1. doi:10.1016/0370-1573(84)90008-5.

[9] H. E. Haber and G. L. Kane, "The Search for Supersymmetry: Probing Physics Beyond the Standard Model", *Phys. Reports* **117** (1987) 75. doi:10.1016/0370-1573(85)90051-1.

[10] R. Barbieri, S. Ferrara, and C. A. Savoy, "Gauge Models with Spontaneously Broken Local Supersymmetry", *Phys. Lett.* **B119** (1982) 343. doi:10.1016/0370-2693(82)90685-2.

[11] S. Dawson, E. Eichten, and C. Quigg, "Search for Supersymmetric Particles in Hadron - Hadron Collisions", *Phys. Rev.* **D31** (1985) 1581. doi:10.1103/PhysRevD.31.1581.

[12] **CMS** Collaboration, V. Khachatryan et al., "Search for Supersymmetry in pp Collisions at 7 TeV in Events with Jets and Missing Transverse Energy", *submitted to Phys. Lett. B* (2011) arXiv:1101.1628v1.

[13] **CMS** Collaboration, V. Khachatryan et al., "First Measurement of the Cross Section for Top-Quark Pair Production in Proton-Proton Collisions at sqrt(s)=7 TeV", *Phys.Lett.* **B695** (2011) 424–443. doi:10.1016/j.physletb.2010.11.058.

[14] G. Kane, "Study of constrained minimal supersymmetry"", *Phys. Rev. D* **49** (1994), no. 11, 6173–6210. doi:10.1103/PhysRevD.49.6173.

[15] A. H. Chamseddine, R. Arnowitt, and P. Nath, "Locally Supersymmetric Grand Unification", *Phys. Rev. Lett.* **49** (Oct, 1982) 970–974. doi:10.1103/PhysRevLett.49.970.

[16] **CMS** Collaboration, G. L. Bayatian et al., "CMS technical design report, volume II: Physics performance", *J. Phys.* **G34** (2007) 995–1579. doi:10.1088/0954-3899/34/6/S01.

[17] T. Sjöstrand, S. Mrenna, and P. Skands, "PYTHIA 6.4 Physics and Manual", *JHEP* **0605** (2006) 026, arXiv:hep-ph/0603175.

[18] J. Alwall, P. Demin, S. de Visscher et al., "MadGraph/MadEvent v4: The New Web Generation", *JHEP* **0709** (2007) 028, arXiv:0706.2334.

[19] **GEANT4** Collaboration, S. Agostinelli et al., "GEANT4: A simulation toolkit", *Nucl. Instrum. Meth.* **A506** (2003) 250–303. doi:10.1016/S0168-9002(03)01368-8.

[20] M. Cacciari, G. P. Salam, and G. Soyez, "The anti-k_t jet clustering algorithm", *JHEP* **04** (2008) 063. doi:10.1088/1126-6708/2008/04/063.

[21] CMS Collaboration, "Jet performance in pp collisions at $\sqrt{s} = 7$ TeV", *CMS-PAS* **JME 10-003** (2010).

[22] CMS Collaboration, "CMS MET Performance in Events Containing Electroweak Bosons from pp Collisions at sqrt(s)=7 TeV", *CMS-PAS* **JME 10-005** (2010).

[23] V. Pavlunin, "Modeling missing transverse energy in V+jets at CERN LHC", *Phys. Rev.* **D81** (2010) 035005. doi:10.1103/PhysRevD.81.035005.

[24] J. A. Aguilar-Saavedra, J. Carvalho, N. Castro et al., "Probing anomalous Wtb couplings in top pair decays", arXiv:hep-ph/0605190v2.

[25] A. Czarnecki, J. G. Korner, and J. H. Piclum, "Helicity fractions of W bosons from top quark decays at NNLO in QCD", *Phys. Rev.* **D81** (2010) 111503, arXiv:1005.2625. doi:10.1103/PhysRevD.81.111503.

[26] CMS Collaboration, "Jet Energy Corrections determination at $\sqrt{s} = 7$ TeV", *CMS-PAS* **JME 10-010** (2010).

[27] CMS Collaboration, "Measurement of CMS luminosity", *CMS-PAS* **EWK-10-004** (2010).

[28] CMS Collaboration, "Commissioning of the Particle-Flow Reconstruction in Minimum-Bias and Jet Events from pp Collisions at 7 TeV", *CMS-PAS* **PFT 10-002** (2010).

[29] I. Bertram, G. Landsberg, J. Linnemann et al., "A Recipe for the construction of confidence limits". FERMILAB-TM-2104, 2000.

[30] B. Allanach, "SOFTSUSY: a program for calculating supersymmetric spectra", *Comput.Phys.Commun.* **143** (2002) 305–331, arXiv:hep-ph/0104145.

[31] W. Beenakker et al., "Squark and Gluino Production at Hadron Colliders", *Nucl.Phys.* **B492** (1997) 51–103. doi:10.1016/S0550-3213(97)00084-9.

[32] P. M. Nadolsky, H.-L. Lai, Q.-H. Cao et al., "Implications of CTEQ global analysis for collider observables", arXiv:0802.0007v3.

[33] **CDF** Collaboration, T. Aaltonen et al., "Inclusive Search for Squark and Gluino Production in $p\bar{p}$ Collisions at $\sqrt{s} = 1.96\ TeV$", *Phys. Rev. Lett.* **102** (Mar, 2009) 121801. doi:10.1103/PhysRevLett.102.121801.

[34] V. Abazov et al., "Search for squarks and gluinos in events with jets and missing transverse energy using 2.1 fb^{-1} of collision data at $\sqrt{s} = 1.96$ TeV", *Physics Letters B* **660** (2008), no. 5, 449 – 457. doi:10.1016/j.physletb.2008.01.042.

[35] LEPSUSYWG, ALEPH, DELPHI, L3 and OPAL experiments, "LSP mass limit in Minimal SUGRA". LEPSUSYWG/02-06.2.

[36] V. Abazov et al., "Search for associated production of charginos and neutralinos in the trilepton final state using 2.3 fb^{-1} of data", *Physics Letters B* **680** (2009), no. 1, 34 – 43. doi:10.1016/j.physletb.2009.08.011.